# Inactivation of human liver bile acid CoA:amino acid *N*-acyltransferase by the electrophilic lipid, 4-hydroxynonenal

**E. M. Shonsey,[1,†] S. M. Eliuk,[†] M. S. Johnson,[§] S. Barnes,[*,†,**,§§] C. N. Falany,[†] V. M. Darley-Usmar,[§,††] and M. B. Renfrow[*,§§]**

Departments of Biochemistry and Molecular Genetics,* Pharmacology and Toxicology,[†] and Pathology,[§] Comprehensive Cancer Center Mass Spectrometry Shared Facility,** Center for Free Radical Biology,[††] and University of Alabama (UAB) Biomedical Fourier Transform-Ion Cyclotron Resonance Mass Spectrometry Laboratory,[§§] University of Alabama at Birmingham, Birmingham, AL 35294

**Abstract The hepatic enzyme bile acid CoA:amino acid *N*-acyltransferase (BAT) catalyzes the formation of amino acid-conjugated bile acids. In the present study, protein carbonylation of BAT, consistent with modification by reactive oxygen species and their products, was increased in hepatic homogenates of apolipoprotein E knock-out mice. 4-Hydroxynonenal (4HNE), an electrophilic lipid generated by oxidation of polyunsaturated long-chain fatty acids, typically reacts with the amino acids Cys, His, Lys, and Arg to form adducts, some of which (Michael adducts) preserve the aldehyde (i.e., carbonyl) moiety. Because two of these amino acids (Cys and His) are members of the catalytic triad of human BAT, it was proposed that 4HNE would cause inactivation of this enzyme. As expected, human BAT (1.6 μM) was inactivated by 4HNE in a dose-dependent manner. To establish the sites of 4HNE's reaction with BAT, peptides from proteolysis of 4HNE-treated, recombinant human BAT were analyzed by peptide mass fingerprinting and by electrospray ionization-tandem mass spectrometry using a hybrid linear ion trap Fourier transform-ion cyclotron resonance mass spectrometer. The data revealed that the active-site His (His362) dose-dependently formed a 4HNE adduct, contributing to loss of activity, although 4HNE adducts on other residues may also contribute.**—Shonsey, E. M., S. M. Eliuk, M. S. Johnson, S. Barnes, C. N. Falany, V. M. Darley-Usmar, and M. B. Renfrow. **Inactivation of human liver bile acid CoA:amino acid *N*-acyltransferase by the electrophilic lipid, 4-hydroxynonenal. *J. Lipid Res.* 2008.** 49: **282–294.**

**Supplementary key words** coenzyme A • post-translational modifications • mass spectrometry

Inflammation plays a major role in many types of liver disease, including cholestasis (1) and both nonalcoholic fatty liver disease (2) and alcoholic fatty liver disease (3). In cholestasis, it has been hypothesized that the inflammatory cytokine pathway that is activated during inflammation causes a functional defect in bile secretion and flow at the hepatocellular level (4). Release of excessive reactive oxygen species (ROS) and reactive nitrogen species (RNS) induces neutrophil and Kupffer cell activation and leads to liver injury (5). ROS and RNS species also play important physiological roles, including release by immune cells to aid in pathogen killing and cell signaling associated with mitochondrial electron transport (6, 7). Normally, the level of oxidative stress is tightly regulated and a balance is maintained between oxidant status and antioxidant capacity. The liver cells' endogenous antioxidant systems consist of enzymes such as superoxide dismutase and catalase (8) that metabolize ROS, and the glutathione-dependent systems that regulate protein thiol modification (9, 10). Nonetheless, these antioxidant systems can be overwhelmed, and the reactive species within the systems can rise to a level at which damage can occur.

An increase in the rate of production of ROS or RNS, or a decrease in their rate of removal, results in direct damage to DNA and proteins, as well as indirectly by reaction with ROS/RNS-modified lipids (11). Modifications of DNA or proteins may be repaired, or they are removed through degradation (11). Patients suffering from various forms of liver disease, including nonalcoholic fatty liver disease (12, 13) and chronic hepatitis C with steatosis (14), show a marked decrease in the level of polyunsaturated fatty acids (PUFAs) and an increase in the products of lipid peroxidation (12, 13).

Lipid peroxidation occurs when PUFAs undergo free radical-initiated oxidation that starts a chain reaction resulting in the formation of electrophilic lipids (15). The most biologically relevant reactive electrophilic lipids are

*Manuscript received 4 May 2007 and in revised form 25 September 2007 and in re-revised form 26 October 2007.*

*Published, JLR Papers in Press, October 27, 2007.*
*DOI 10.1194/jlr.M700208-JLR200*

[1] To whom correspondence should be addressed.
e-mail: eshonsey@uab.edu

the 2-alkenals, 4-hydroxy-2-alkenals, and ketoaldehydes (15). One of the most thoroughly studied of these is 4-hydroxynonenal (4HNE). Kawamura et al. (16) showed an increase in levels of 4HNE protein adducts through immunohistochemical staining by use of a polyclonal 4HNE antibody in patients with primary biliary cirrhosis. Seki et al. (17) detected 4HNE protein adducts in the hepatocytes of patients suffering from alcoholic liver disease by use of a monoclonal 4HNE antibody.

Although several studies have reported an increase in levels of protein-aldehyde adduct formation in hepatocytes, relatively few modifications of specific proteins have been characterized (18–20). To identify cellular targets affected by inflammatory responses, models of sepsis have been employed to identify the genes that undergo differential regulation. In a study of late sepsis induced for 18 h by a cecal ligation and puncture (CLP) method in rats, three upregulated genes and six downregulated genes were found (21). The six downregulated genes in rat liver were hydroxysteroid dehydrogenase, EST/189895/mouse RNase4, IF1, albumin, α2u-globulin, and rat bile acid CoA:amino acid *N*-acyltransferase (rBAT) (21). Furutani et al. (22) also showed downregulation of rBAT following partial hepatectomy and during sepsis. BAT is responsible for the conjugation of bile acids with amino acids. This is a two-step reaction in which bile acids are first converted to CoA thioesters by bile acid CoA ligase and are then conjugated with an amino acid by BAT (23, 24).

The loss of BAT message is thought to play a role in the disturbance of bile acid metabolism that contributes to the liver failure observed in the CLP model of sepsis (21). This leads to the hypothesis that a decrease in BAT activity would play a role in the overall failure of the liver as well. Similarly, in a case in which excessive lipid peroxidation occurs, modification of the enzyme by electrophilic lipids may result in a decrease in activity of human BAT (hBAT) that could also contribute to liver damage and failure. This raises the following questions: does 4HNE decrease BAT activity and would protein-aldehyde adduct formation cause disruption of protein structure significant enough to affect the enzyme's activity?

hBAT belongs to a protein family of α/β fold hydrolases and has an enzymatic mechanism based on a catalytic triad, Cys-His-Asp (24). Two of these amino acid residues (His and Cys) are potential targets for modification by electrophilic lipids. Mutation studies have demonstrated that replacement of each member of the catalytic triad eliminates the activity of the enzyme (24). hBAT activity has been detected in both the peroxisomes and the cytosol of hepatocytes, indicating that BAT is localized in these two regions of the cell (25–29).

Traditionally, posttranslational modifications have been identified on proteins through the use of specific antibodies; although this technique is useful in gaining an understanding of overall modification within a system, it cannot provide unequivocal information on the actual site of modification, particularly because of an antibody's epitope bias. More recently, mass spectrometry (MS) has become a standard tool in the identification of adduct formation. 4HNE adducts are identified by an increase in the expected mass of proteolytic peptides by either a Michael adduct (156.1150 Da), a Schiff base adduct (138.1045 Da), or a 2-pentylpyrrole adduct (120.0939 Da) (30–32). The presence of an aldehyde adduct is then confirmed by use of tandem mass spectrometry (MS/MS), which allows direct assignment of the modification to a specific amino acid (32). Fourier transform-ion cyclotron resonance mass spectrometry (FT-ICR MS) provides high resolution and high mass accuracy and has become widely used in the characterization of posttranslational modifications, including phosphorylation (33, 34), glycosylation (35, 36), and others (37, 38). The combination of FT-ICR MS with the rapid MS/MS scan rate of a two-dimensional linear ion trap provides a powerful tool for the investigation of site-specific posttranslational modifications.

In this study, hBAT was incubated with a range of 4HNE concentrations, producing changes in the activity of the enzyme that were correlated with the extent of posttranslational modifications induced by 4HNE. FT-ICR MS/MS was performed on proteolytic digests of the untreated and 4HNE-treated hBAT to identify sites of modification. The potential for these modifications to occur in vivo was assessed in the liver in the apolipoprotein E (apoE) knock-out mouse using protein carbonyl formation as a surrogate index of modification by reactive aldehydes. This animal model of hypercholesterolemia is associated with increased oxidative stress and protein modification (39). Increased protein carbonyls were associated with BAT in the apoE knock-out mouse liver homogenates compared with those from wild-type mice, thus providing a potential mechanism linking oxidative stress and regulation of BAT activity.

## MATERIALS AND METHODS

### Materials

Sodium chloride, Trizma base, Luria Bertani broth (LB), ampicillin, isopropylthio-β-D-galactoside (IPTG), and 1-butanol were purchased from Fisher Scientific (Norcross, GA). Biotin was purchased from Research Organics (Cleveland, OH). 4HNE was purchased from Calbiochem (San Diego, CA). Trypsin (sequencing grade) and Softlink avidin (avi) were purchased from Promega (Madison, WI). Chymotrypsin and protease inhibitor cocktail were purchased from Roche (Nutley, NJ). Biotin hydrazide was purchased from Pierce Chemical Co. (Rockford, IL). Diethylaminoethyl (DEAE) -Sephacryl was obtained from Bio-Rad (Hercules, CA). Chloramphenicol was purchased from Acros Organics (Belgium). Bugbuster solution was obtained from Novagen (San Diego, CA). Cholyl CoA was synthesized as described by Shah and Staple (40). Its purity was assessed by its absorbance at 230 nm and by negative-ion electrospray ionization mass spectrometry (ESI MS) (*m/z* 1,159 $[M\text{-}H]^-$; *m/z* 579 $[M\text{-}2H]^{2-}$; there was no *m/z* 407 ion that would indicate the presence of unreacted cholic acid).

### Methods

*Preparation of mouse liver homogenates.* Fresh livers from apoE knock-out and C57/BL6 mice were minced and homogenized in a glass tissue grinder using ice-cold isolation medium contain-

ing 0.25 M sucrose, 1 mM EDTA, and 5 mM Tris-HCl, pH 7.4. Nuclear debris and cellular debris were removed by centrifugation at 3,000 *g* for 10 min at 4°C.

*Biotin hydrazide labeling of protein carbonyls and protein electrophoresis.* Liver homogenate (50 μg as determined by Bradford assay) was reacted with biotin hydrazide (1 mM in phosphate-buffered saline) at 37°C for 1 h and then precipitated with 4 vols methanol, followed by 3 vols water, followed by 1 vol chloroform.

Samples were centrifuged for 20 min at 16,000 *g* at 4°C. Protein pellets were allowed to air dry at 37°C. Controls were treated under identical conditions. The precipitated protein was subjected to SDS-12.5% polyacrylamide gel electrophoresis according to Laemmli (41). Dried protein samples were resolubilized in 25 μl 2× SDS-PAGE sample buffer (20 μl β-mercaptoethanol/ml buffer) and 25 μl water to give a 1 mg/ml protein concentration. The hydrazide-linked proteins (15 μg) were separated by SDS-PAGE (12.5% polyacrylamide at 100 V) followed by Western blotting (overnight at 35 V). The membrane was blocked with 5% blotting-grade blocker nonfat dry milk (Bio-Rad) in TBS-T (0.25 M Tris, 35 mM NaCl, 27 mM KCl, 0.5% Tween 20) for 2 h at room temperature. The membranes were then incubated with streptavidin HRP conjugated to goat anti-rabbit IgG (Amersham) at 1/10,000 for 1 h at room temperature. The signal was detected using chemiluminescence (Pierce). Quantitation was done using AlphaEase FC software (AlphaInnotech; San Leandro, CA), and the amount of carbonyl adduct formed was calculated using a biotinylated cytochrome-C internal standard (42).

The precipitated biotin hydrazide-labeled protein was also subjected to 2D-electrophoresis. The proteins were focused on linear pH 5–8 isoelectrofocusing strips in the first dimension and then resolved by electrophoresis on an SDS-12.5% polyacrylamide gel. The proteins were transferred to Immobilon-FL polyvinylidene fluoride membrane (Millipore), which was blocked with Odyssey blocking buffer. The blot was then probed with a polyclonal rabbit anti-mouse BAT antibody (43), followed with streptavidin Alexa fluor 680 conjugate and a fluorescent secondary antibody, Alexa fluor 800 goat anti-rabbit IgG (Invitrogen). These two tags fluoresce at different wavelengths, which permits simultaneous analysis of two targets on the same blot. The membrane was scanned with a fluorescence imager (Odyssey LiCor Infrared Imager) at wavelengths of both 700 nm and 800 nm to detect both fluorescent components.

*In vitro expression and biotinylation of hBAT in* Escherichia coli. *Escherichia coli* cells (BL-21) transformed with a modified pET21a+ expression vector encoding hBAT with a C-terminal avi-tag (24), as well as an expression vector containing the gene for biotin ligase, were incubated in 5 ml cultures of LB at 37°C and shaken at 180 rpm for 18 h. The 5 ml cultures contained 5 μl of 0.1 mg/ml ampicillin and 5 μl of 0.01 mg/ml chloramphenicol. The cultures were placed in 400 ml LB containing 400 μl of 0.1 mg/ml ampicillin and 400 μl of 0.01 mg/ml chloramphenicol. The cultures were incubated for 2.5 h at 37°C with shaking at 250 rpm. After 2.5 h, expression was induced through the addition of IPTG to a final concentration of 400 μM. To achieve biotinylation, biotin was added to a final concentration of 250 μM. The cultures were incubated at 30°C with shaking at 200 rpm for a further 3 h. Following the incubation time, the cultures were centrifuged at 3,000 *g* for 20 min at 25°C to obtain a bacterial pellet.

*Purification of hBAT.* Cell pellets were resuspended in 5 ml Bugbuster solution and 5 μl benzonase per milligram bacterial protein, and incubated at room temperature for 30 min for lysis. One half of a protease inhibitor cocktail tablet (Roche) was also added. The lysates were centrifuged at 140,000 *g* for 40 min at 4°C. The supernate was applied to a DEAE-Sephacryl column (20 ml bed volume) that had been preequilibrated with 5 bed volumes of 50 mM Tris-HCl, pH 8.5, containing 5 mM NaCl. The DEAE column was then washed with 10 bed volumes of 50 mM Tris-HCl, pH 8.5, to remove unbound proteins. Elution of bound proteins was performed by use of a 40 ml gradient of 5–1,000 mM NaCl in 50 mM Tris-HCl, pH 8.5, collecting 2 ml fractions. The fractions were tested for BAT activity, and the active fractions were applied to a Softlink avi column preequilibrated with 5 bed volumes of 5 mM NaCl in 50 mM Tris-HCl, pH 8.5. The avi column was washed with 20 bed volumes of 50 mM Tris-HCl, pH 8.5, to remove nonbound proteins. Biotinylated hBAT was eluted from the column by use of 3 bed volumes of 50 mM Tris-HCl, pH 8.5, containing 10 mM biotin.

*Preparation of 4HNE-modified hBAT.* hBAT was modified by 4HNE using a method described by Isom et al. (32). Purified hBAT (160 pmol in a total volume of 100 μl) was mixed in a glass tube with 50 mM potassium phosphate buffer, pH 7.4, and a range of 4HNE concentrations (4 μM to 128 μM) in ethanol and incubated at 4°C for 1 h. The reaction was terminated by quenching with 1 mM histidine (for the hBAT enzyme assay) or 5 μl 0.1% (v/v) formic acid (for protein mass spectrometry experiments). A vehicle control was performed with the addition of ethanol in place of 4HNE and incubation under the same conditions.

*Radioassay of BAT activity.* hBAT enzyme activity was assayed as described by Johnson, Barnes, and Diasio (44). Briefly, 12.5 μl of 0.8 mM cholyl-CoA, 12.5 μl of $^{3}$H-taurine (2 μCi/mmol), 12.5 μl of 100 mM potassium phosphate buffer, pH 8.4, and 2 pmol of enzyme were mixed in an Eppendorf tube and incubated at 37°C for 15 min. The reaction was terminated by the addition of 0.5 ml of butanol-saturated $K_2HPO_4$, pH 2.0, containing 2% w/v SDS. The mixture was vortexed thoroughly, and then 0.5 ml of water-saturated butanol was added. Following a 1 min vortex, the mixture was centrifuged at 2,000 *g* for 5 min at room temperature. The butanol layer was transferred to a clean Eppendorf tube and backwashed with 0.5 ml of the potassium phosphate buffer. The mixture was vortexed for 1 min and centrifuged at 2,000 *g* for 5 min at room temperature. An aliquot (250 μl) of the butanol layer was mixed with 4.5 ml of scintillation fluid, and the radioactivity was measured in a liquid scintillation counter.

*Proteolysis of hBAT and matrix-assisted laser desorption ionization time-of-flight mass spectrometry peptide mass fingerprinting.* Both the native and modified forms of hBAT (30 μl of a 1.6 μM solution) were digested with either trypsin (10 μl of a 12.5 ng/μl solution) at 37°C or chymotrypsin (10 μl of a 12.5 ng/μl solution) at room temperature overnight. The peptide digests were analyzed by matrix-assisted laser desorption ionization time-of-flight mass spectrometry (MALDI-TOF MS). Aliquots (1 μl) were mixed with 3 μl of a saturated solution of α-cyano-4-hydroxycinnamic acid in a 50/50 mixture of 0.1% trifluoroacetic acid and acetonitrile. An aliquot (1 μl) of the mixture was spotted on the MALDI target plate and allowed to dry for 5 min. The molecular ions were generated by a pulsed $N_2$ laser at 337 nm and analyzed by delayed extraction in the positive reflector ion mode using an Applied Biosystems (Foster City, CA) Voyager DE-PRO mass spectrometer with an acceleration voltage of 20 kV. The acquired spectra, an accumulation of 300 laser shots, were analyzed using

DataExplorer® (Applied Biosystems). Internal calibration was carried out using one of the digestive enzyme autolysis peaks, *m/z* 2,162.05 for trypsin and *m/z* 1,528.58 for chymotrypsin. Spectra were baseline corrected and noise filtered.

*Liquid chromatography-ESI FT-ICR MS/MS analysis of 4HNE-modified peptides.* The proteolytic digests of hBAT (20 pmol) were separated by nanoLC (Eksigent; Dublin, CA) on a 15 cm × 75 μm inner diameter reverse-phase $C_{18}$ column with a linear gradient of 5–95% acetonitrile in 0.1% formic acid at a flow rate of 200 nl/min$^{-1}$. FT-ICR MS analysis was performed on a linear quadrupole ion trap (LTQ) FT ICR hybrid mass spectrometer (LTQ FT; Thermo Electron, San Jose, CA). Eluted tryptic and chymotryptic peptides were electrosprayed at 2 kV. Peptide fragmentation was induced by collision-induced dissociation (CID) in the ion trap, and fragment ions were also analyzed in the ion trap. The LTQ FT mass spectrometer was operated in a "top three" data-dependent acquisition mode. The mass spectrometer was set to switch between an FT-ICR MS full scan (200 *m/z*–2,000 *m/z*) followed by successive FT-ICR MS single-ion monitoring scans and LTQ MS/MS scans of the three most abundant precursor ions in the FT-ICR MS full scan as determined by the Xcalibur software (Thermo Electron). Dynamic exclusion was enabled after a repeat count of three for a period of 90 s.

*Data analysis.* The MALDI-TOF MS peaks were compared with in silico digests obtained from ProteinProspector (http://prospector.ucsf.edu) for both hBAT and the digestive enzymes in order to eliminate any autolysis peaks as potential modified hBAT peptides. The liquid chromatography-electrospray ionization (LC-ESI) LTQ MS/MS data were searched against a custom FASTA sequence database containing hBAT, as well as unrelated human proteins as a negative control, by use of the TurboSEQUEST algorithm within Bioworks 3.2 (Thermo Electron). Monoisotopic precursor and fragment ion masses were searched with a mass tolerance of 5 ppm and 5 ppm, respectively. For identification of 4HNE-modified peptides, the TurboSEQUEST searches were amended to search for the mass additions of 156.1150 Da, 138.1045 Da, and 120.0939 Da for Michael, Schiff base, and 2-pentylpyrrole adducts, respectively. Additionally, FT-ICR MS spectra were extracted out of each sample data set for manual identification of modifications based on high mass accuracy. The modified peptides were manually validated by their absence in the unmodified FT-ICR MS spectra; a mass accuracy cut-off of 2 ppm was used.

## RESULTS

### Formation of BAT protein carbonyls is increased in the liver of the apo $E^{-/-}$ mouse

Homogenates were prepared from the livers of apoE knock-out and C57/BL6 mice. Protein carbonyls were then measured by their derivatization using biotin hydrazide, followed by 1D-electrophoretic separation of the proteins and assessment of the biotin signal with fluorescent streptavidin. Under these conditions, protein carbonyls could be formed from ROS and/or by modification with reactive lipid aldehydes such as 4HNE (45, 46). There was a significant increase in protein carbonylation ($P < 0.05$) in the liver homogenates of apoE knock-out mice compared with C57/BL6 mice (**Fig. 1A**). Analysis by 2D-isoelectric focusing/SDS-PAGE and Coomassie blue staining demonstrated that equal protein loadings had occurred (Fig. 1B). Western blot analysis with a specific polyclonal anti-mouse BAT antibody revealed that mouse BAT was present in several isoforms with decreasing isoelectric points in both the C57/BL6 and the apoE knock-out mice (Fig. 1D). In apoE knock-out liver homogenates, more acidic isoforms of mouse BAT were present (Fig. 1D, right panel). Visualization with fluorescent streptavidin demonstrated that many liver proteins were carbonylated (Fig. 1C). Colocalization of the biotin signals and those immunoreactive to BAT occurred for the apoE knock-out mice, but not for the C57/BL6 mice (Fig. 1E).

### Purification of hBAT

hBAT, subcloned into a modified pET21a+ vector that contains a C-terminal avi-tag allowing for affinity purification, was coexpressed with biotin ligase, which adds biotin to the avi-tag during protein expression. Following overexpression in *E. coli* BL-21 cells, the recombinant protein was purified on a DEAE-Sephacryl column by anion exchange chromatography. hBAT eluted at 120 mM NaCl, with a recovery of approximately 90% of its enzyme activity. The active fractions were pooled, and proteins were subjected to affinity chromatography on a Softlink avi column. The Softlink avi column uses competitive elution with free biotin, allowing the eluted enzyme to retain activity. Following the affinity purification, 69% of enzyme activity was recovered. The purification resulted in a 0.2 mg/ml solution of greater than 95% pure hBAT-avi that gave a single band by SDS-PAGE analysis (**Fig. 2**). The purified form of hBAT was used in subsequent activity and mass spectrometry experiments.

### Inactivation of hBAT-avi following modification with 4HNE

Purified hBAT (1.6 μM) was incubated with 4HNE over a range of concentrations to determine its effect on enzyme activity. hBAT (1.6 μM) was incubated with increasing concentrations of 4HNE (4 μM, 8 μM, 16 μM, 32 μM, and 64 μM) for 1 h. The 4HNE concentrations were chosen to mimic physiologically relevant levels of 4HNE within the liver, which have been reported in ranges from the nanomolar to millimolar level (47). Reduction of hBAT activity was observed to be dose dependent (**Fig. 3**). At the two highest levels of 4HNE treatment (128 μM and 64 μM), hBAT activity was not detected. At 32 μM 4HNE, the treated protein retained 5.0 ± 3.5% activity when compared with untreated hBAT. At the lower concentrations of 4HNE (16 μM, 8 μM, and 4 μM), reduction in enzyme activity was less severe (25.7 ± 3.1%, 61.9 ± 7.8%, and 84.2 ± 8.6%, respectively). These results indicate that 4HNE-dependent modifications occur to the protein that reduce the enzyme activity in a dose-dependent manner. Next, we determined the sites of modification by 4HNE in hBAT.

### 4HNE modification of hBAT peptide mass fingerprinting

To assess the presence of 4HNE modifications, both tryptic and chymotryptic digests of native and modified

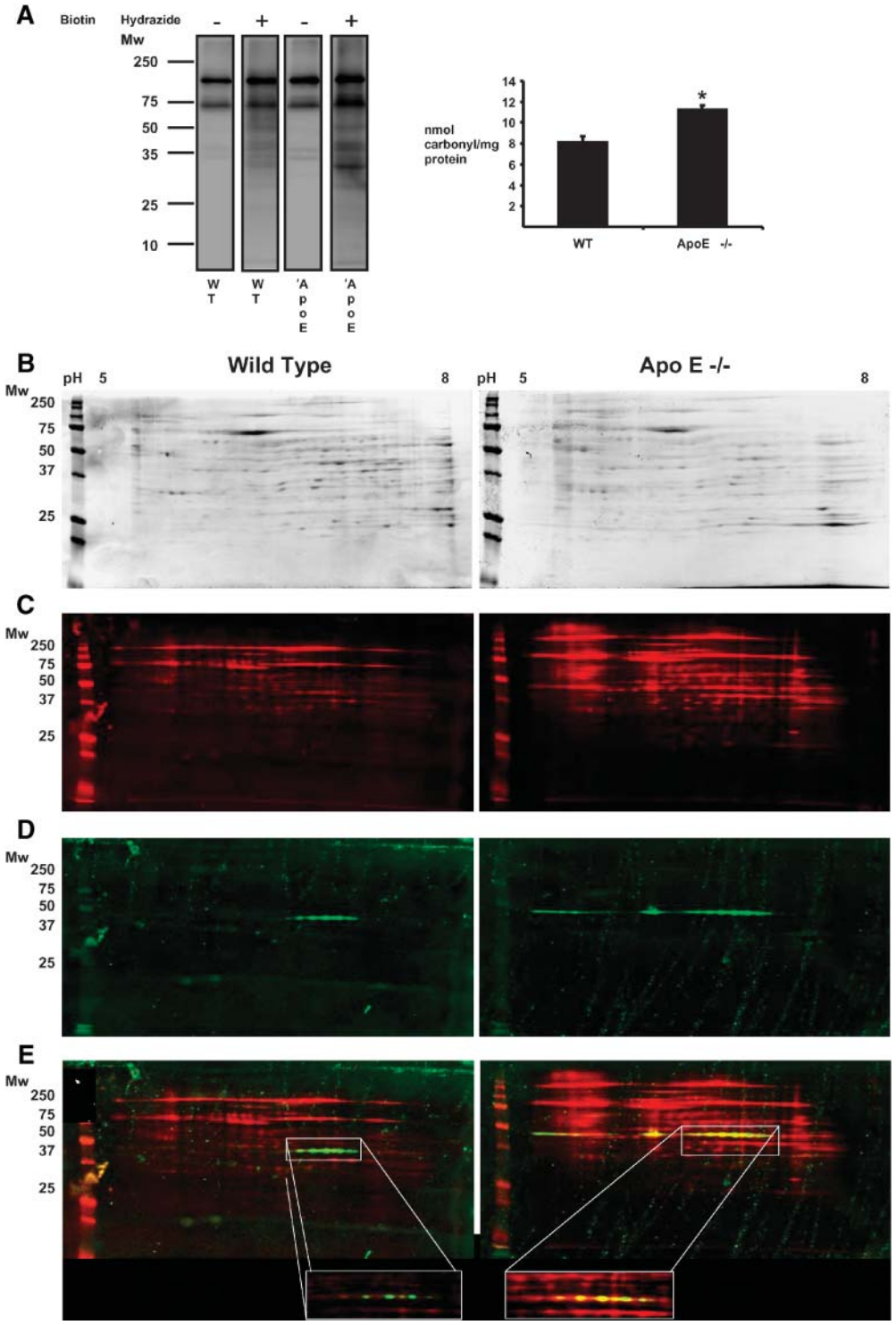


**Fig. 1.** Increased oxidation of mouse bile acid CoA:amino acid *N*-acyltransferase (BAT) in the liver of apolipoprotein E (apoE) knock-out mice. A: Wild-type and apoE knock-out mouse liver homogenates (50 μg protein) were treated with 1 mM biotin hydrazide. Proteins (15 μg) were separated by SDS-polyacrylamide gel electrophoresis, followed by Western blot analysis. Biotin incorporation corresponding to the degree of carbonyl formation was quantified using biotinylated cytochrome C as a standard. Results are expressed as mean ± SE, n = 3. $*P < 0.05$ relative to wild-type. B–E: Liver homogenate (50 μg) was subjected to 2D isoelectric focusing SDS-PAGE. The proteins were resolved in the first dimension over a linear pH range of 5–8 and separated in the second dimension using a 12.5% polyacrylamide gel and either stained with comassie blue (B) or transferred to a polyvinylidene difluoride membrane and blocked with 5% milk. Biotin hydrazide-labeled proteins (red) were detected with fluorescent-streptavidin (C), and mouse BAT (green) was detected with a polyclonal rabbit anti-mouse BAT antibody followed by a fluorescent goat anti-rabbit antibody (D). Cofluorescence, indicating oxidation of BAT on the merged gel images, is shown in yellow (E).

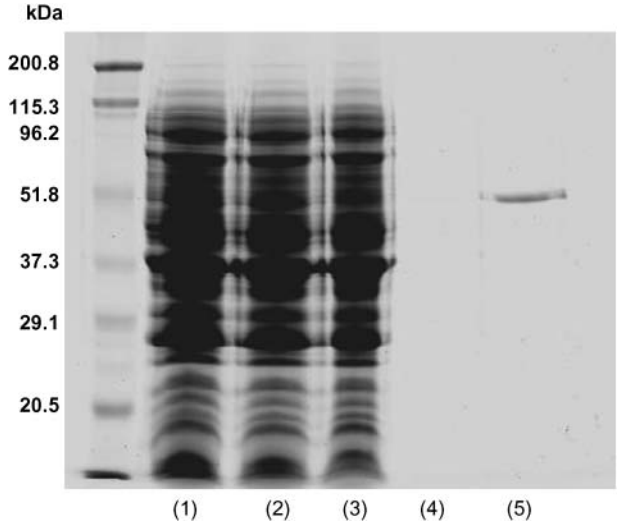


**Fig. 2.** Recombinant human BAT (hBAT)-avidin (avi) isolated from *Escherichia coli*. Recombinant hBAT-avi was isolated from bacterial cytosol (lane 1) in a two-step purification. Cytosol was initially loaded onto a DEAE column and eluted with NaCl gradient. Fractions retaining hBAT activity (pooled fractions, lane 2) were then loaded onto an avi column (lane 3, flow through) and washed with 50 mM Tris, pH 8.0 (lane 4). hBAT-avi was competitively eluted with biotin, resulting in >95% purification (lane 5).

hBAT were analyzed by use of MALDI-TOF MS. The spectra obtained for the modified peptides were compared against the spectra obtained for the peptides derived from the unreacted hBAT to identify new peaks that correlated to mass shifts associated with 4HNE modifications. **Figure 4** shows the tryptic peptide mass fingerprint MALDI-TOF MS spectra for untreated hBAT (Fig. 4A), as well as hBAT following modification with 1 mM 4HNE (Fig. 4B).

Comparison of the native hBAT MALDI-TOF mass spectrum with the 4HNE-modified BAT spectrum revealed the presence of a new ion species (*m/z* 1,478) in the modified BAT spectrum that corresponded to a 156 Da mass addition to the ion at *m/z* 1,322. This represents a putative 4HNE adduct to the peptide AHAEQAIGQLKR (residue numbers 335–347). Because 4HNE modification to a lysine or an arginine could prevent trypsin cleavage (32), a second proteolytic enzyme (chymotrypsin) was used to decrease the chance of missing such modifications.

**Figure 5** shows both the native (Fig. 5A) and modified (Fig. 5B) chymotryptic MALDI-TOF MS for hBAT. As in the tryptic mass spectrum, new ion species were detected in the modified spectrum that corresponded to 156 Da mass additions to unmodified ions. These peptide ions, at *m/z* 1,195.7, 1,320.6, 1,719.9, and 1,914.5 in the modified mass spectrum represent putative 4HNE adducts to hBAT. For all four peptide ions (K345-W353, K93-F101, H271-L284, and R51-L66), the mass difference corresponded to a single Michael adduct to the peptides; however, each of these peptides contains more than one possible site of 4HNE adduct formation. This initial analysis of 4HNE adducts in the hBAT showed that modifications occurred to hBAT and led to the putative identification of five sites of modification; however, the precise residues could not be assigned.

### Analysis of 4HNE-modified hBAT peptides by use of LC-ESI LTQ FT-ICR MS and MS/MS

After initial MALDI-TOF MS analysis indicated the presence of 4HNE adducts on hBAT peptides, sites of modification were localized for tryptic and chymotryptic digests of 4HNE-modified hBAT by use of LC-ESI LTQ FT-ICR MS/MS. This analysis was performed over a range of 4HNE concentrations (8 μM–128 μM). The data were analyzed by use of the TurboSEQUEST algorithm and by accurate mass assignment of modified peptides from the FT-ICR mass spectra. The high resolution and high mass accuracy (<2 ppm) of FT-ICR MS allowed manual inspection of the mass spectra of tryptic and chymotryptic hBAT peptides for the known mass increases of 156.1150 Da, 138.1045 Da, and 120.0939 Da, corresponding to 4HNE Michael, Schiff base, and 2-pentylpyrrole additions, respectively. At 128 μM 4HNE, 14 modifications were identified on 8 different peptides. At the lowest concentration of 4HNE (8 μM), 7 modifications were found on 5 peptides. The results for all concentrations of 4HNE are listed in **Table 1**.

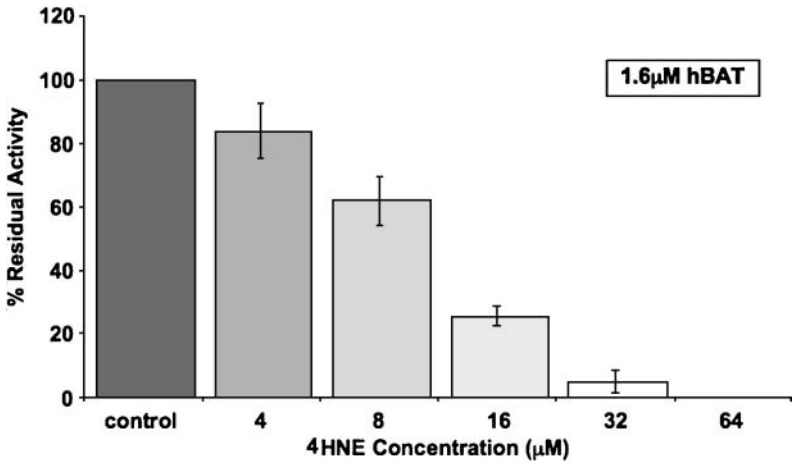


**Fig. 3.** Inhibition of hBAT activity by 4-hydroxynonenal (4HNE). hBAT (1.6 μM) was pretreated by incubation with 4HNE (4 μM–64 μM) for 1 h at 4°C, and then the mixture was quenched with 1.0 mM histidine. The remaining enzyme activity of hBAT was measured by use of a radioassay (see Materials and Methods), with cholyl CoA (0.8 mM) and 1,2-$^{3}$H-taurine (0.1 μCi; 1 mM) as substrates. Each bar represents the average of three independent measurements of hBAT-avi activity, with the results reported as a percentage of the activity measured for unmodified hBAT-avi. Error bars indicate ± SD.

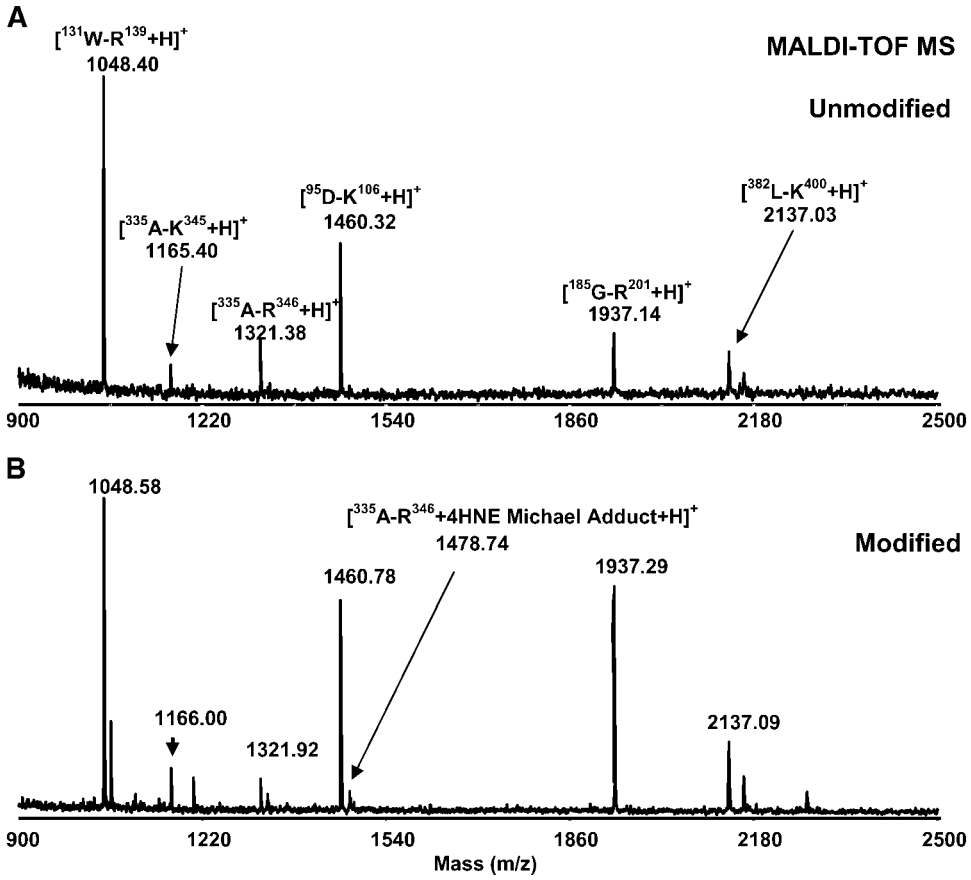


**Fig. 4.** Matrix-assisted laser desorption ionization time-of-flight mass spectrometry (MALDI-TOF MS) peptide mass fingerprints of native and 4HNE-modified hBAT following trypsin digestion. After treatment with 1 mM 4HNE, tryptic digests of the untreated protein (A) and the 4HNE-modified hBAT (B) were analyzed by MALDI-TOF MS. Several hBAT tryptic peptides were identified in the unmodified spectra (A). An additional tryptic peptide corresponding to $[^{335}\text{A-R}^{346}+156]^{+}$ was detected in the 4HNE-treated hBAT spectrum.

MS/MS can unambiguously map specific sites of post-translational modification (35), including amino acids modified by 4HNE adduction (32). The LTQ FT mass spectrometer fragments the tryptic and chymotryptic peptides by CID in the ion trap. CID of peptide ions results in the fragmentation of the peptides at the amide bonds to produce *b*- and *y*-type fragment ions. When 1.6 μM hBAT was reacted with 32 μM 4HNE, ten different sites of modification were localized with a mass accuracy of 2 ppm by both TurboSEQUEST and manual inspection of the FT-ICR mass spectra (Table 1). **Figure 6** shows the LTQ MS/MS spectrum of the triply charged *m/z* 625.6877 ion from the chymotrypsin digest of 4HNE-treated hBAT. The parent mass from the FT-ICR spectrum (not shown) indicated that the ion species corresponded to the hBAT chymotryptic peptide $[^{271}\text{HGQIHQPLPHSAQL}^{283}$ + 2 Michael adducts + $2\text{H}]^{2+}$ (1,875.0487 theoretical mass, 1,875.04856 observed mass, 0.07 ppm error). Inspection of the LTQ MS/MS spectrum confirmed the peptide sequence with the addition of two Michael adducts as follows. From the N terminus, $b_1$–$b_4$ ions are present with a mass increase of 156.1, corresponding to a 4HNE Michael adduct on the H271 residue. The remaining *b* ions ($b_5$, $b_6$, $b_8$, and $b_9$) show no additional mass increase of 156.1. This eliminates H274 as a site of 4HNE modification. From the C terminus, the initial $y_2$ ion corresponds to the first two amino acids, leucine and glutamine. The subsequent observed *y* ions ($y_6$–$y_9$) have a mass increase of 156.1, corresponding to a 4HNE Michael adduct on H279. The remaining *y* ions ($y_{10}$–$y_{12}$), containing both H279 and H274, show no additional mass increase of 156.1. This is in agreement with analysis of the N-terminal *b* ions. The combination of fragment ions unambiguously assigns the two sites of 4HNE Michael adducts as H271 and H279.

**Figure 7** shows the LTQ MS/MS spectrum for a second doubly charged $927.4885^{2+}$ ion from the chymotrypsin digest of 4HNE-treated hBAT. The parent mass from the FT-ICR spectrum (not shown) indicated that the ion species corresponded to the hBAT chymotryptic peptide $[^{356}\text{SYPGAGHLIEPPYSPL}^{371}$ + Michael adduct + $2\text{H}]^{2+}$ (1,853.9689 theoretical mass, 1,853.9684 observed mass, 0.27 ppm error). This peptide includes H362, a member of the catalytic triad. The LTQ MS/MS spectrum confirmed the peptide sequence with the addition of a single Michael adduct. CID product ions from both N- and C-terminal directions, $b_8$–$b_{14}$ and $y_{10}$–$y_{14}$, confirm the ex-

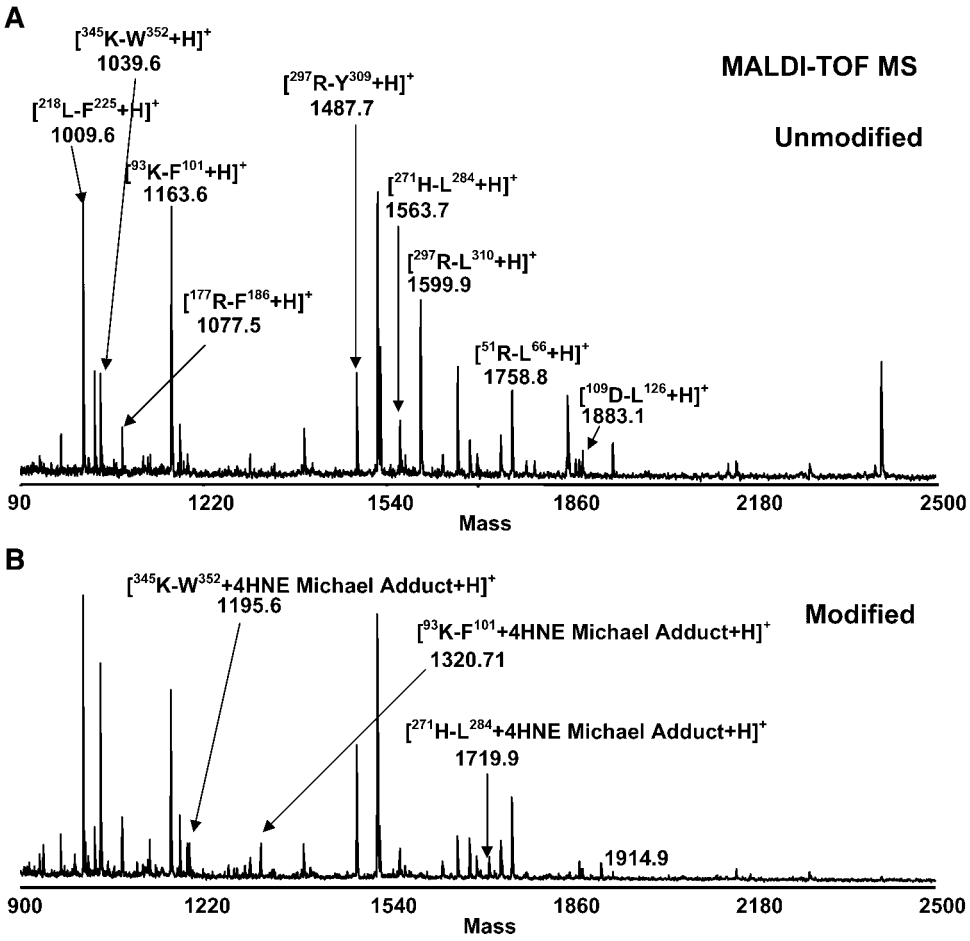


**Fig. 5.** MALDI-TOF MS peptide mass fingerprints of native and 4HNE-modified hBAT following chymotrypsin digestion. hBAT was treated with 4HNE as described in the legend to Fig. 3. Following that reaction, the untreated protein (A) and the 4HNE-modified hBAT (B) were digested with chymotrypsin and analyzed by use of MALDI-TOF MS. Modified peptides are labeled in B.

pected sequence with the addition of 156.1 to H362. This mass addition is not seen on $b_3$ and $b_5$ ions N-terminal to the addition or $y_3$ and $y_5$–$y_9$ ions C-terminal to the addition. This unambiguously localizes the 4HNE Michael adduct to the H362 residue. Table 1 shows the residues modified at each concentration of 4HNE treatment.

**Sequence coverage by two proteolytic digests**

Analysis of 4HNE-modified peptides was performed by tryptic and chymotryptic digests of hBAT and indicated that 49 out of the 55 sites that could be modified by 4HNE were observed. MS analysis of the hBAT trypsin digest yielded peptides corresponding to 70% of the hBAT

TABLE 1. 4HNE-modified peptides identified by LTQ FT-ICR MS/MS in hBAT at 4HNE concentrations from 128 μM to 8 μM

| | Modified Amino Acid | | | | |
|---|---|---|---|---|---|
| | 4HNE Concentration | | | | |
| Peptide | *128 μM* | *64 μM* | *32 μM* | *16 μM* | *8 μM* |
| AHAEQAIGQLKR | H336 | H336 | H336 | H336 | H336 |
| RLHWGGEVIPHAAAQEHAWK | H397 | H397 | H397 | H397 | |
| AQGQFLFIVGEGDKTINSK | K329, K334 | K329, K334 | K329, K334 | K329, K334 | K329, K334 |
| MIQLTATPVSALVDEPVHIR | H18 | H18 | | | |
| RANEFGEVDLNHASSLGGDYMGVHPMGLFWSLKPEK | H62, H74 | H62, H74 | H62, H74 | H62, H74 | H62 |
| HGQIHQPLPHSAQL | H271, H274, H279 | H271, H274, H279 | H271, H274, H279 | H271, H274, H279 | H271, H279 |
| NNWTLLSYPGAGHLIEPPYSPLCCASTTHDLR | H362, C372, C373, H378 | H362 | H362 | H362 | H362 |

hBAT, human bile acid CoA:amino acid *N*-acyltransferase; 4HNE, 4-hydroxynonenal; LTQ FT-ICR MS/MS, linear quadrupole ion trap Fourier transform-ion cyclotron resonance tandem mass spectrometry.

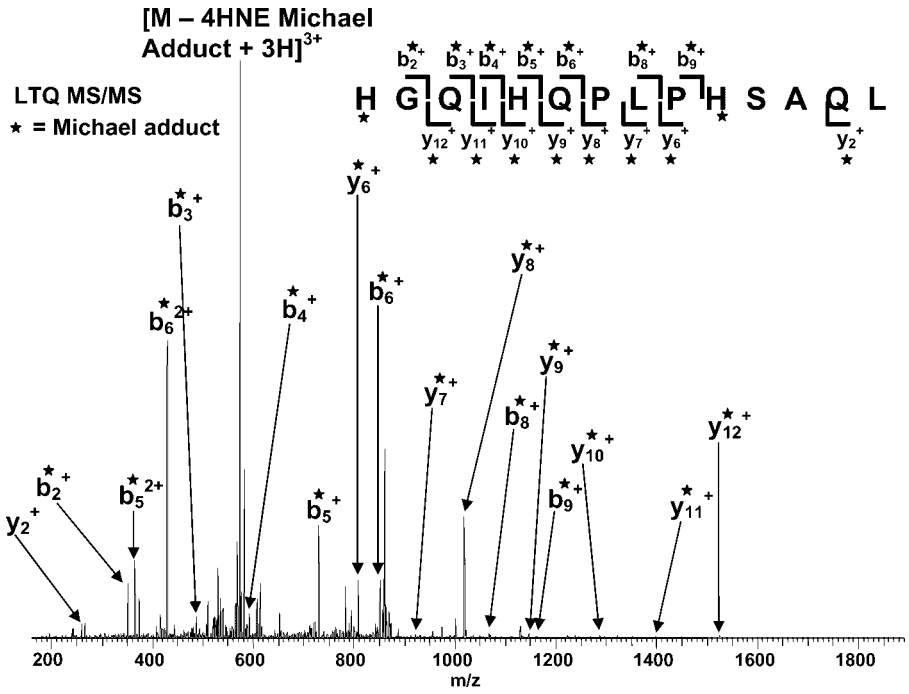


**Fig. 6.** Linear quadrupole ion trap tandem mass spectrometry (LTQ MS/MS) spectrum of the triply charged 4HNE-modified hBAT peptide $NH_2$-SYPGAGHLIEPPYSPL-COOH at *m/z* 625.688. A single LTQ MS/MS spectrum from the liquid chromatography-electrospray ionization LTQ Fourier transform-ion cyclotron resonance mass spectrometry (LC-ESI LTQ FT-ICR MS) analysis of 4HNE-modified hBAT-avi digested with chymotrypsin successfully localized a site of modification. Peptide backbone bonds (9 of 13) are cleaved. Sites of 4HNE modification were identified from a series of differentially Michael adduct (156.1) -modified fragment ions. The fragment ions uniquely localize two sites of 4HNE Michael adduction, to His271 and His279, and eliminate His274 as a modified site. N-terminal fragment ions (*b*) and C-terminal fragment ions (*y*) are indicated above and below the hBAT-avi chymotryptic peptide sequence, respectively. Stars, Michael adducts.

amino acid sequence and localized 10 sites of modification. Although the inclusion of an hBAT chymotrypsin digest resulted in only a modest increase in sequence coverage, the difference in the number of observed sites of adduct formation was significant. Analysis of the chymotrypsin digest of hBAT increased the sequence coverage modestly, to 78.7%, but identified four additional sites of modification.

### Semiquantitation of 4HNE-modified His362

The ion abundance of the chymotryptic peptide $^{356}$SYPGAGHLIEPPYSPL$^{371}$ containing the 4HNE-modified H362 versus the same peptide in an unmodified form was compared at all levels of 4HNE treatment. The abundances of each pair of ions were normalized against two peptides (*m/z* 639.8212 and *m/z* 653.8654) that were not modified at any level of 4HNE treatment. The semiquantitative analysis demonstrated a dose-dependent effect on the level of modified and unmodified peptide detected. At 128 μM 4HNE, there was no detectable level of unmodified peptide (**Fig. 8**). At 64 μM 4HNE, there was a low level of unmodified peptide in comparison to the modified form of the peptide. The level of unmodified peptide increased as the concentration of 4HNE decreased. At 8 μM 4HNE, the lowest concentration used, the modified form of the peptide decreased, whereas the level of unmodified peptide increased.

## DISCUSSION

The present study demonstrates that carbonylation of the important liver enzyme BAT occurs in a model of oxidative stress, the apoE knock-out mouse. Furthermore, the electrophilic lipid 4HNE, a product of oxidative stress in the liver, causes a dose-dependent reduction of the activity of recombinantly expressed human liver BAT. More importantly, even at the lowest concentrations of 4HNE, amino acids that are part of or adjacent to the active site are modified, as determined by high-resolution FT-ICR-MS. These experiments, therefore, also provide structural insight into the hBAT active site.

Bile acid amidation with the amino acids glycine and taurine is a vital process in normal hepatobiliary and gastrointestinal functions. Amidated bile acids form mixed micelles in both the biliary tract and the lumen of the small intestine. Mutations in hBAT have been identified in patients who have decreased levels of amidated bile acids (47). This results in a variety of symptoms associated with a decrease in the ability to absorb fat and fat-soluble

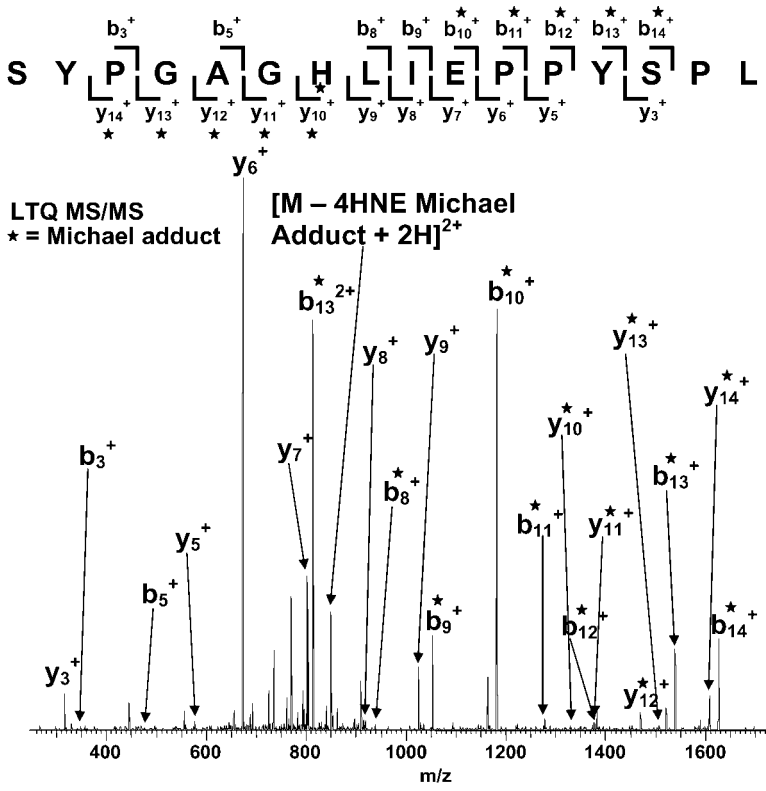


**Fig. 7.** LTQ MS/MS spectrum of the 4HNE-modified doubly charged hBAT peptide $NH_2$-SYPGAGH-LIEPPYSPL-COOH at *m/z* 927.088. Peptide backbone bonds (13 of 15) are broken (notation as in Fig. 6). The fragment ions unambiguously localize the 4HNE Michael adduct to the His362 active site residue. This and six other sites were modified across all concentrations of 4HNE treatment (Table 1).

vitamins. In some forms of liver disease, including cholestasis (1), nonalcoholic fatty liver disease (2), alcoholic fatty liver disease (3), and atherosclerosis, oxidative stress plays a key role in the progression of the disease. Subsequently, lipid peroxidation increases the level of 4HNE within the liver, and hBAT and other liver enzymes are at a higher risk of modification by 4HNE. In the apoE knock-out mouse, 4HNE production has been observed through increased immunohistochemical staining using a 4HNE-specific antibody and is decreased by treatment with antioxidants, which also have a beneficial effect on the development of the disease (48). In the present study, there was increased protein carbonyl formation in the mouse liver in apoE knock-out mice compared with wild-type mice. It was accompanied by marked carbonyl formation associated with different isoforms of BAT in apoE knock-out mouse liver, but not in the C57/BL6 mice.

To pursue the effect of an electrophilic lipid, in vitro experiments were carried out with 4HNE and recombinantly expressed hBAT. At high concentrations of 4HNE (aldehyde-to-protein ratio of 80:1), BAT activity was completely abolished. Over the range from 4 μM–32 μM 4HNE, a dose-dependent decrease in hBAT activity was observed, with 80% of the activity remaining at an aldehyde-to-protein ratio of 2.5:1 (Fig. 2). This dose-dependent effect was characterized at the molecular level by use of LC-ESI LTQ FT-ICR MS and MS/MS to identify and localize sites of modification.

4HNE modifies amino acids that contain nucleophilic groups, including histidines, lysines, and cysteines, through the formation of Michael adducts (49). Lysine residues also form both Schiff bases and 2-pentylpyrrole adducts with 4HNE (30, 31). Recently, 4HNE has also been shown to modify arginine residues, forming 2-pentylpyrrole adducts (32). We hypothesize that as the inflammatory process progresses, hBAT activity is diminished, leading to an increase of unconjugated bile acids in the liver, a decrease in bile flow, and a decrease in conjugated bile acids within the intestinal tract. All of these pathologies could contribute to increased liver damage in pathologies associated with increased hepatic ROS/RNS.

At the highest level of 4HNE treatment of hBAT, a total of 14 distinct modifications were found. As expected, the number of sites of modification decreased as the concentration of 4HNE treatment decreased (Table 1). The observed modifications can be evaluated in the context of what is known about the structure of hBAT, specifically the active site. hBAT belongs to a protein family of α/β fold hydrolases that are characterized by an enzyme mechanism based on a Cys-His-Asp catalytic triad (50). Previous mutational studies have identified Cys235, Asp328, and His362 as the residues critical to hBAT activity (24). These three residues are located on three loops between a β-strand and an α-helix. These loops are hypothesized to fold, creating a substrate binding pocket. This α/β fold structure was first characterized in the crystal structure of

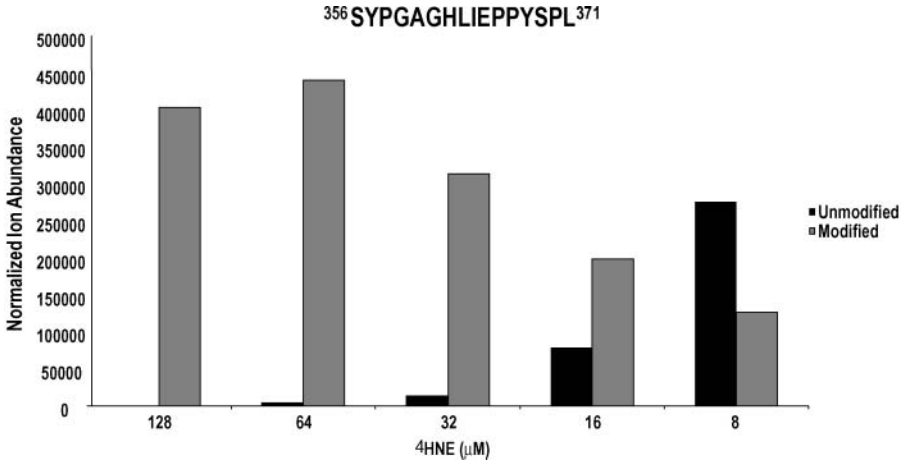


**Fig. 8.** Semiquantitation of the modified and unmodified peptide containing the active site residue His362. The relative abundances of the chymotryptic modified and unmodified His362-containing peptides were compared across all concentrations of 4HNE treatment. To account for variability in the amount of chymotryptically digested hBAT-avi loaded onto the column, individual ion abundances in each sample were normalized against two control peptides within the same LC-ESI LTQ FT-ICR MS analysis (*m/z* 639.8212 and 514.7689) that were lacking in amino acids that could be modified by 4HNE. As the concentration of 4HNE was increased, the ion abundance of the unmodified peptide decreased and the modified peptide increased in a dose-dependent manner.

dienelactone hydrolase (51). As many as 11 enzymes have been identified as members of this family, based on three-dimensional crystal structures and the presence of a catalytic triad consisting of a nucleophile-His acid-amino acid triad positioned on the loops of the protein (50, 51). Sequence similarity searches using NCBI BLAST have found significant similarity between hBAT, dienelactone hydrolase, and other α/β hydrolases (24).

Within hBAT, the catalytic triad is in the C-terminal half of the protein. Two of the residues are susceptible to 4HNE modification (Cys235 and His362). At all levels of 4HNE incubation where hBAT activity was reduced (Fig. 3), His362 was modified with a 4HNE Michael adduct. Mutation studies that replaced the active site His with an Ala residue abolished enzyme activity (24). This suggests that modification of the His by 4HNE would have a similar result on the activity of the enzyme. It was observed, however, that partial hBAT activity remained intact, even with the presence of the modified His362. Semiquantitative analysis of the His362-modified peptide across all concentrations of 4HNE revealed that there is a dose-dependent change in the ratio of modified to unmodified His362-containing peptide (Fig. 8). The relationship between the forms of the His362-containing peptide is correlated with hBAT activity levels (Figs. 3, 8). This demonstrates the cumulative effect that prolonged exposure to 4HNE can have on the enzyme. Of the 55 possible residues that can be modified by 4HNE within hBAT, the modification of the active site His362 at even low ratios of 4HNE demonstrates the active site's accessibility to oxidative modification/damage. The remaining modifications can be evaluated in the context of dividing hBAT into two halves, the C-terminal half that contains the catalytic triad and the N-terminal half that has not been reported as being vital to hBAT enzymatic activity.

Fewer modifications were found on the N-terminal half of the protein, with modifications at the highest level of 4HNE treatment on His18, His62, and His74. These are hypothesized to lie within the unstructured region at the N-terminus of the protein, and as such would probably be more susceptible to posttranslational modification, owing to increased accessibility of the ROS to that region of the protein. These are the only modifications seen within the N-terminal half of the protein, with only two additional potential sites of modification unaccounted for in the sequence coverage. The localization of fewer modifications to the N-terminal half of the protein may be due to poor accessibility of potential sites of modification, whereas in the C-terminal half of the protein, the accessibility to the residues increases with the location of the binding pocket within this region of the protein.

At the highest level of 4HNE modification, nine residues in close proximity to the members of the catalytic triad are also modified. These include 4HNE Michael adducts on His271, His274, His279, Lys329, Lys334, His336, Cys372, Cys373, and His378. Among these additional sites of modification, Cys372 has been shown to be essential to hBAT enzyme activity (24). Mutation of Cys372 to Ala372 decreased the *N*-acyltransferase activity of the enzyme, but with a small amount of activity remaining (24). Cys372, Cys373, and His378 are all in the catalytic histidine-containing loop. Modification of these sites is only observed at the highest concentration of 4HNE treatment. Although their modification may result in further reduction in hBAT activity, they are probably not the sites that 4HNE adduction would damage first. In contrast, Lys329, Lys334, His336, His271, and His279 are modified at all concentrations of 4HNE treatment. Lys329, Lys334, and His336 are in the hypothesized acid loop, with Lys329 directly adjacent to the catalytic triad member Asp328.

His271 and His 279 are hypothesized to be in the loop between the sixth β-sheet and fourth α-helix. Modification of these residues with the same level of susceptibility as the catalytic triad member His362 would suggest that they have a role in substrate access to the active site. Therefore, damage to these sites could have as much significance in terms of reduction of hBAT activity as does modification to the active site His362 itself. These modifications may block substrate accessibility to the essential members of the catalytic triad directly, by infiltrating the binding pocket of the protein, or indirectly, by shifting the relative position of the members of the catalytic triad through structural disturbance of the loops containing them. Of these five amino acids, we hypothesize that modification of Lys329 in such close proximity to the catalytic triad may have the most significant role in the inhibition of enzyme activity. The addition of a bulky Michael adduct could disrupt the charge relay mechanism that hBAT uses for its conjugation activity. This modification, in combination with the His362 modification at all concentrations, may combine to explain how 4HNE blocks hBAT activity, even at relatively low levels of 4HNE.

Based on the location of the majority of the modifications in hBAT and the subsequent activity analysis, the C-terminal half of the protein is important for its enzymatic function. Posttranslational modifications occurring within the binding pocket of an enzyme have the potential to block substrate access to the active site residues specifically, or to completely block access to the binding pocket. Whether the modifications observed in hBAT are blocking substrate access, or the charge relay mechanism that hBAT uses (24), needs further examination. Studies also need to be performed to determine the residues within hBAT that play a role in the binding pocket of the protein in order to better understand the role that the modifications observed are playing in the inhibition of hBAT activity.

This study was supported by Grants-in-aid from the National Institute of Diabetes, Digestive and Kidney Diseases, R01 DK-46390-08 (S.B.), and from the National Heart, Lung and Blood Institute, PO1 HL-70610 (V.M.D-U.). The mass spectrometers were purchased following Shared Instrumentation Awards from the National Center for Research Resources, S10 RR-13795 and S10 RR-17261 (S.B.), and support from the University of Alabama at Birmingham School of Medicine. Funds for the operation of the University of Alabama at Birmingham Comprehensive Cancer Center Mass Spectrometry Shared Facility were provided by a National Cancer Institute Core Support Grant, P30 CA-13148-35 (E. Partridge). Funds for the operation of the University of Alabama at Birmingham Biomedical FT-ICR MS Laboratory were provided in part by the Supporters of the University of Alabama at Birmingham Comprehensive Cancer Center and the Department of Biochemistry and Molecular Genetics.

## REFERENCES

1. Guicciardi, M. E., and G. J. Gores. 2005. Cholestatic hepatocellular injury: what do we know and how should we proceed. *J. Hepatol.* **42:** 297–300.
2. Adams, L. A., and P. Angulo. 2005. Recent concepts in non-alcoholic fatty liver disease. *Diabet. Med.* **22:** 1129–1133.
3. Lieber, C. S. 2004. Alcoholic fatty liver: its pathogenesis and mechanism of progression to inflammation and fibrosis. *Alcohol.* **34:** 9–19.
4. Trauner, M., P. Fickert, and R. E. Stauber. 1999. Inflammation-induced cholestasis. *J. Gastroenterol. Hepatol.* **14:** 946–959.
5. Jaeschke, H., G. J. Gores, A. I. Cederbaum, J. A. Hinson, and D. Pessayre. 2002. Mechanisms of hepatotoxicity. *Toxicol. Sci.* **65:** 166–176.
6. Filomeni, G., and M. R. Ciriolo. 2006. Redox control of apoptosis: an update. *Antioxid. Redox Signal.* **8:** 2187–2192.
7. Valko, M., D. Leibfritz, J. Moncol, M. T. Cronin, and M. Mazur. 2007. Free radicals and antioxidants in normal physiological functions and human disease. *Int. J. Biochem. Cell Biol.* **39:** 44–84.
8. Mates, J. M., C. Perez-Gomez, and I. Nunez de Castro. 1999. Antioxidant enzymes and human diseases. *Clin. Biochem.* **32:** 595–603.
9. Masella, R., R. Di Benedetto, R. Varì, C. Filesi, C. Giovannini. 2005. Novel mechanisms of natural antioxidant compounds in biological systems: involvement of glutathione and glutathione-related enzymes. *J. Nutr. Biochem.* **16:** 577–586.
10. Murrant, C. L., and M. B. Reid. 2001. Detection of reactive oxygen and reactive nitrogen species in skeletal muscle. *Microsc. Res. Tech.* **55:** 236–248.
11. Stadtman, E. R., and R. L. Levine. 2000. Protein oxidation. *Ann. N. Y. Acad. Sci.* **899:** 191–208.
12. Videla, L. A., R. Rodrigo, J. Araya, and J. Poniachik. 2004. Oxidative stress and depletion of hepatic long-chain polyunsaturated fatty acids may contribute to nonalcoholic fatty liver disease. *Free Radic. Biol. Med.* **37:** 1499–1507.
13. Araya, J., R. Rodrigo, L. A. Videla, L. Thielemann, M. Orellana, P. Pettinelli, and J. Poniachik. 2004. Increase in long-chain polyunsaturated fatty acid n - 6/n - 3 ratio in relation to hepatic steatosis in patients with non-alcoholic fatty liver disease. *Clin. Sci. (Lond.).* **106:** 635–643.
14. Kitase, A., K. Hino, T. Furutani, M. Okuda, T. Gondo, I. Hidaka, Y. Hara, Y. Yamaguchi, and K. Okita. 2005. In situ detection of oxidized n-3 polyunsaturated fatty acids in chronic hepatitis C: correlation with hepatic steatosis. *J. Gastroenterol.* **40:** 617–624.
15. Uchida, K. 2000. Role of reactive aldehyde in cardiovascular diseases. *Free Radic. Biol. Med.* **28:** 1685–1696.
16. Kawamura, K., Y. Kobayashi, F. Kageyama, T. Kawasaki, M. Nagasawa, S. Toyokuni, K. Uchida, and H. Nakamura. 2000. Enhanced hepatic lipid peroxidation in patients with primary biliary cirrhosis. *Am. J. Gastroenterol.* **95:** 3596–3601.
17. Seki, S., T. Kitada, H. Sakaguchi, K. Nakatani, and K. Wakasa. 2003. Pathological significance of oxidative cellular damage in human alcoholic liver disease. *Histopathology.* **42:** 365–371.
18. Yamagami, K., Y. Yamamoto, M. Kume, Y. Ishikawa, Y. Yamaoka, H. Hiai, and S. Toyokuni. 2000. Formation of 8-hydroxy-2'-deoxyguanosine and 4-hydroxy-2-nonenal-modified proteins in rat liver after ischemia-reperfusion: distinct localization of the two oxidatively modified products. *Antioxid. Redox Signal.* **2:** 127–136.
19. Khan, M. F., X. Wu, U. R. Tipnis, G. A. Ansari, and P. J. Boor. 2002. Protein adducts of malondialdehyde and 4-hydroxynonenal in livers of iron loaded rats: quantitation and localization. *Toxicology.* **173:** 193–201.
20. Hartley, D. P., K. L. Kolaja, J. Reichard, and D. R. Petersen. 1999. 4-Hydroxynonenal and malondialdehyde hepatic protein adducts in rats treated with carbon tetrachloride: immunochemical detection and lobular localization. *Toxicol. Appl. Pharmacol.* **161:** 23–33.
21. Hsieh, Y. C., C. Hsu, R. C. Yang, P. Y. Lee, H. K. Hsu, and Y. M. Sun. 2004. Isolation of bona fide differentially expressed genes in the 18-hour sepsis liver by suppression subtractive hybridization. *Shock.* **21:** 549–555.
22. Furutani, M., S. Arii, H. Higashitsuji, M. Mise, M. Fukumoto, S. Takano, H. Nakayama, M. Imamura, and J. Fujita. 1995. Reduced expression of kan-1 (encoding putative bile acid-CoA-amino acid N-acyltransferase) mRNA in livers of rats after partial hepatectomy and during sepsis. *Biochem. J.* **311:** 203–208.
23. Shonsey, E. M., M. Sfakianos, M. Johnson, D. He, C. N. Falany, J. Falany, D. J. Merkler, and S. Barnes. 2005. Bile acid coenzyme A:amino acid N-acyltransferase in the amino acid conjugation of bile acids. *Methods Enzymol.* **400:** 374–394.
24. Sfakianos, M. K., L. Wilson, M. Sakalian, C. N. Falany, and S. Barnes. 2002. Conserved residues in the putative catalytic triad of human bile acid coenzyme A:amino acid N-acyltransferase. *J. Biol. Chem.* **277:** 47270–47275.

25. Styles, N. A., J. L. Falany, S. Barnes, and C. N. Falany. 2007. Quantification and regulation of the subcellular distribution of bile acid CoA:amino acid N-acyltransferase activity in rat liver. *J. Lipid Res.* **48:** 1305–1315.
26. Solaas, K., A. Ulvestad, O. Soreide, and B. F. Kase. 2000. Subcellular organization of bile acid amidation in human liver: a key issue in regulating the biosynthesis of bile salts. *J. Lipid Res.* **41:** 1154–1162.
27. He, D., S. Barnes, and C. N. Falany. 2003. Rat liver bile acid CoA:amino acid N-acyltransferase: expression, characterization, and peroxisomal localization. *J. Lipid Res.* **44:** 2242–2249.
28. O'Byrne, J., M. C. Hunt, D. K. Rai, M. Saeki, and S. E. Alexson. 2003. The human bile acid-CoA:amino acid N-acyltransferase functions in the conjugation of fatty acids to glycine. *J. Biol. Chem.* **278:** 34237–34244.
29. Pellicoro, A., F. A. van den Heuvel, M. Geuken, H. Moshage, P. L. Jansen, and K. N. Faber. 2007. Human and rat bile acid-CoA:amino acid N-acyltransferase are liver-specific peroxisomal enzymes: implications for intracellular bile salt transport. *Hepatology.* **45:** 340–348.
30. Liu, Z., P. E. Minkler, and L. M. Sayre. 2003. Mass spectroscopic characterization of protein modification by 4-hydroxy-2-(E)-nonenal and 4-oxo-2-(E)-nonenal. *Chem. Res. Toxicol.* **16:** 901–911.
31. Fenaille, F., P. A. Guy, and J. Tabet. 2003. Study of protein modification by 4-hydroxy-2-nonenal and other short chain aldehydes analyzed by electrospray ionization tandem mass spectrometry. *J. Am. Soc. Mass Spectrom.* **14:** 215–226.
32. Isom, A. L., S. Barnes, L. Wilson, M. Kirk, L. Coward, and V. Darley-Usmar. 2004. Modification of cytochrome C by 4-hydroxy-2-nonenal: evidence for histidine, lysine, and arginine-aldehyde adducts. *J. Am. Soc. Mass Spectrom.* **15:** 1136–1147.
33. Chalmers, M. J., K. Hakansson, R. Johnson, R. Smith, J. Shen, M. R. Emmett, and A. G. Marshall. 2004. Protein kinase A phosphorylation characterized by tandem Fourier transform ion cyclotron resonance mass spectrometry. *Proteomics.* **4:** 970–981.
34. Chalmers, M. J., J. P. Quinn, G. T. Blakney, M. R. Emmett, H. Mischak, S. J. Gaskell, and A. G. Marshall. 2003. Liquid chromatography-Fourier transform ion cyclotron resonance mass spectrometric characterization of protein kinase C phosphorylation. *J. Proteome Res.* **2:** 373–382.
35. Renfrow, M. B., H. J. Cooper, M. Tomana, R. Kulhavy, Y. Hiki, K. Toma, M. R. Emmett, J. Mestecky, A. G. Marshall, and J. Novak. 2005. Determination of aberrant O-glycosylation in the IgA1 hinge region by electron capture dissociation Fourier transform-ion cyclotron resonance mass spectrometry. *J. Biol. Chem.* **280:** 19136–19145.
36. Dalpathado, D. S., J. Irungu, E. P. Go, V. Y. Butnev, K. Norton, G. R. Bousfield, and H. Desaire. 2006. Comparative glycomics of the glycoprotein follicle stimulating hormone: glycopeptide analysis of isolates from two mammalian species. *Biochemistry.* **45:** 8665–8673.
37. Cooper, H. J., M. H. Tatham, E. Jaffray, J. K. Heath, T. T. Lam, A. G. Marshall, and R. T. Hay. 2005. Fourier transform ion cyclotron resonance mass spectrometry for the analysis of small ubiquitin-like modifier (SUMO) modification: identification of lysines in RanBP2 and SUMO targeted for modification during the E3 autoSUMOylation reaction. *Anal. Chem.* **77:** 6310–6319.
38. Hakansson, K., H. J. Cooper, M. R. Emmett, C. E. Costello, A. G. Marshall, and C. L. Nilsson. 2001. Electron capture dissociation and infrared multiphoton dissociation MS/MS of an N-glycosylated tryptic peptic to yield complementary sequence information. *Anal. Chem.* **73:** 4530–4536.
39. Whitman, S. C., S. L. Hazen, D. B. Miller, R. A. Hegele, J. W. Heinecke, and M. W. Huff. 1999. Modification of type III VLDL, their remnants, and VLDL from apoE-knockout mice by p-hydroxyphenylacetaldehyde, a product of myeloperoxidase activity, causes marked cholesteryl ester accumulation in macrophages. *Arterioscler. Thromb. Vasc. Biol.* **19:** 1238–1249.
40. Shah, P. P., and E. Staple. 1968. Synthesis of coenzyme A esters of some bile acids. *Steroids.* **12:** 571–576.
41. Laemmli, U. K. 1970. Cleavage of structural proteins during the assembly of the head of bacteriophage T4. *Nature.* **227:** 680–685.
42. Landar, A., J. Y. Oh, N. M. Giles, A. Isom, M. Kirk, S. Barnes, and V. M. Darley-Usmar. 2006. A sensitive method for the quantitative measurement of protein thiol modification in response to oxidative stress. *Free Radic. Biol. Med.* **40:** 459–468.
43. Falany, C. N., H. Fortinberry, E. H. Leiter, and S. Barnes. 1997. Cloning, expression, and chromosomal localization of mouse liver bile acid CoA:amino acid N-acyltransferase. *J. Lipid Res.* **38:** 1139–1148.
44. Johnson, M. R., S. Barnes, and R. B. Diasio. 1989. Radioassay of bile acid coenzyme A:glycine/taurine: N-acyltransferase using an n-butanol solvent extraction procedure. *Anal. Biochem.* **182:** 360–365.
45. Yoo, B. S., and F. E. Regnier. 2004. Proteomic analysis of carbonylated proteins in two-dimensional gel electrophoresis using avidin-fluorescein affinity staining. *Electrophoresis.* **25:** 1334–1341.
46. Roe, M. R., H. Xie, S. Bandhakavi, and T. J. Griffin. 2007. Proteomic mapping of 4-hydroxynonenal protein modification sites by solid-phase hydrazide chemistry and mass spectrometry. *Anal. Chem.* **79:** 3747–3756.
47. Carlton, V. E., B. Z. Harris, E. G. Puffenberger, A. K. Batta, A. S. Knisely, D. L. Robinson, K. A. Strauss, B. L. Shneider, W. A. Lim, G. Salen, et al. 2003. Complex inheritance of familial hypercholanemia with associated mutations in TJP2 and BAAT. *Nat. Genet.* **34:** 91–96.
48. Takaya, T., S. Kawashima, M. Shinohara, T. Yamashita, R. Toh, N. Sasaki, N. Inoue, K. Hirata, and M. Yokoyama. 2006. Angiotensin II type 1 receptor blocker telmisartan suppresses superoxide production and reduces atherosclerotic lesion formation in apolipoprotein E-deficient mice. *Atherosclerosis.* **186:** 402–410.
49. Esterbauer, H., R. J. Schaur, and H. Zollner. 1991. Chemistry and biochemistry of 4-hydroxynonenal, malonaldehyde and related aldehydes. *Free Radic. Biol. Med.* **11:** 81–128.
50. Holmquist, M. 2000. Alpha/beta-hydrolase fold enzymes: structures, functions and mechanisms. *Curr. Protein Pept. Sci.* **1:** 209–235.
51. Pathak, D., K. L. Ngai, and D. Ollis. 1988. X-ray crystallographic structure of dienelactone hydrolase at 2.8 A. *J. Mol. Biol.* **204:** 435–445.